Biodegradable Network Polyesters from Gluconolactone and Citric Acid

Naoto Tsutsumi,* Masaya Oya, and Wataru Sakai

Department of Polymer Science & Engineering, Kyoto Institute of Technology, Matsugasaki, Sakyo, Kyoto 606-8585, Japan

Received February 27, 2004; Revised Manuscript Received May 16, 2004

ABSTRACT: This paper presents biodegradable polyesters prepared from gluconolactone (G) and citric acid (C) with various molar ratios of G to C, 1/4, 1/3, 1/2, 1/1, 2/1, 3/1, and 4/1. Corresponding polyesters were named as GC14, GC13, GC12, GC11, GC21, GC31, and GC41, respectively. Prepolymers, prepared at 165 °C by a melt polycondensation, were cast from tetrahydrofuran solution and postpolymerized at 180 °C for various periods of time to form a network. The resultant films were transparent, flexible, and insoluble in organic solvents. The polyesters obtained were characterized by infrared spectroscopy, wide-angle X-ray diffraction analysis, density measurement, differential scanning calorimetry (DSC), dynamic mechanical analysis, thermomechanical analysis (TMA), and tensile test. The degree of reaction was estimated from the ratio between absorbance due to the stretching vibration of the hydroxyl group and that of the methylene group. Enzymatic degradability was performed at 37 °C in a buffer solution with *Rhizopus delemar* lipase. The degree of enzymatic degradation was decreased with decreasing C content in the polymers as follows: GC14 > GC13 > GC12 > GC11 > GC21 ≈ GC31 ≈ GC41 ≈ 0, which corresponded to the decrease of the average molecular weight between cross-linked sites. Two transition temperatures were measured on thermograms in DSC and TMA curves. The higher transition temperature was ascribed to the release of restricted motion in the molecule pinned by the cross-linked sites. The lower transition temperature was attributed to the transition due to the segmental molecular motion of the ester linkage. Large Young's modulus and tensile strength were obtained in the dried state of GC31 and GC21, respectively. Water absorbed in the polymer matrix was worked as a plasticizer, and largely depressed Young's modulus and tensile strength were measured for the sample in water.

Introduction

Extensive studies on biodegradable polymers have been reported in recent years. Energy and environmental problems also accelerate the development of biodegradable polymers and the enzyme-catalyzed production of polymers. Biodegradable polymers due to hydrolysis, poly(glycolic acid) (PGA), and poly(lactic acid) (PLA) are used in both in vitro and in vivo applications. Enzymatic biodegradable polymers, poly(butylene succinate) (PBS) and poly(hydroxyl butylic acid) (PHB), have potential applications in the field of common plastics.

Up to now, biodegradable network polyesters have been reported in the literature.[1−17] Photoinitiated cross-linking of the biodegradable poly(propylene fumarate) was reported.[1,2] In situ cross-linkable macroporous biodegradable poly(propylene fumarate-*co*-ethylene glycol) hydrogels were synthesized and characterized.[3] The in vitro cytotoxicity of injectable and biodegradable poly(propylene fumarate)-based networks was investigated.[4] We have reported the preparation and the properties of various biodegradable network polyester films from several polyhydric alcohols and aliphatic dicarboxylic acids with various methylene lengths.[7−13] It has been found that the thermal and the mechanical properties as well as the biodegradability behavior are varied depending markedly on the chemical structures as well as the length of the methylene chains. Another type of network polymer, some biodegradable cross-linked polymers, has been prepared to enhance the thermal and the mechanical properties. Poly(butylene succinate)s were cross-linked with peroxide[14] or radiation,[15] and cross-linked polymers were prepared on the basis of triethoxysilane-terminated polylactide oligomers.[16] Biodegradable injectable and in situ cross-linkable polymer networks based upon di(propylene fumarate)-dimethacrylate and polycaprolactone trimethacrylate were prepared and characterized.[17]

Renewable and natural resources-based biodegradable polymers are environmentally useful for the establishment of the recycled system. Gluconolactone is derived from natural resources. Citric acid, also derived from natural resources, is used as cross-linking agent.[18,19] Biodegradable network polyester can be prepared from gluconolactone and citric acid. After the biodegradation of the polyester, monomeric components of gluconolactone and citric acid return back to natural resources. This kind of recycled system is a useful way for keeping environmentally renewable and sustainable resources. In this paper, biodegradable polyesters were prepared from gluconolactone and citric acid. The effect of the molecular structures on enzymatic degradation and the thermal and mechanical properties were investigated.

Experimental Section

Materials. Gluconolactone (G), supplied from Fujisawa Pharmaceutical Co. Ltd., and citric acid (C), commercially available, were used as received. The molecular structures of G and C are shown in Figure 1.

Preparation of Prepolymers. Prepolymers of G and C were prepared using a melt polycondensation method. A mixture of G and C was heated in a stream of nitrogen at 165 °C for 3 h for a G/C molar ratio of 1/1 and for 5 h for other molar ratio of G/C = 1/4, 1/3, 1/2, 2/1, 3/1, and 4/1. Polymer with G/C = 1/4, 1/3, 1/2, 1/1, 2/1, 3/1, and 4/1 was denoted GC14, GC13, GC12, GC11, GC21, GC31, and GC41, respectively.

Film Preparation and Postpolymerization. Prepolymers were cast on an aluminum substrate from a 17 wt % tetrahydrofuran (THF) solution and followed by heating at

* To whom correspondence should be addressed. E-mail: tsutsumi@kit.ac.jp.

10.1021/ma049607g CCC: $27.50
Published on Web 07/14/2004

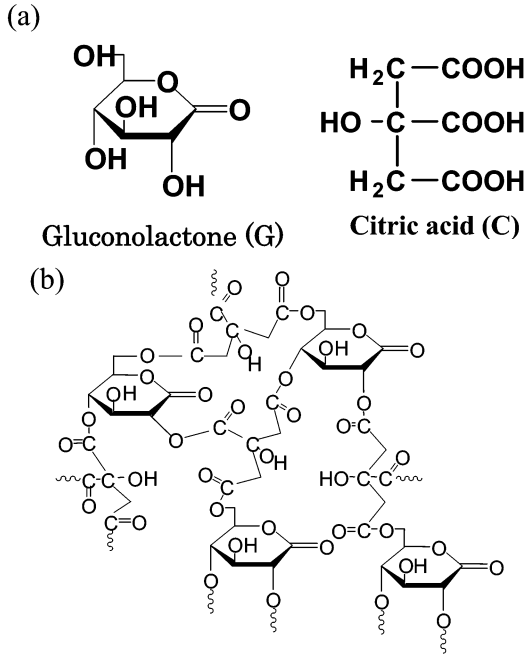

Figure 1. (a) Chemical structures of materials. (b) An example of the molecular structure of GC11 for complete progress of reaction.

room temperature for 2 h and additionally at 65 °C for 2 h for complete drying of the THF solvent. Dried cast films were postpolymerized in a nitrogen atmosphere at 180 °C for 2 h except for the case of 3 h for GC13 and 1 h for GC12. The determination of the postpolymerization time will be discussed later. After postpolymerization, the film was immersed in hydrochloride solution to dissolve aluminum substrate and was stored in a desiccator over silica gel.

Characterization. Fourier transform infrared (FT-IR) spectra were recorded on a Perkin-Elmer model Spectrum GX FTIR spectrometer equipped with a microscope. Wide-angle X-ray scattering (WAXS) was performed with a Toshiba model ADG-301 X-ray diffractometer with nickel-filtered Cu Kα radiation. Modulated differential scanning calorimetry (MDSC) was carried out on a TA Instruments DSC 2920 differential scanning calorimeter with a heating rate of 2 °C/min and modulation period of 60 s with an amplitude of 0.796 °C in a nitrogen atmosphere. Thermomechanical analysis (TMA) was performed in a penetration mode under a pressure of 10 kg/cm^2 and a heating rate of 20 °C/min in a nitrogen atmosphere, using a Seiko model TMA-100 thermomechanical analyzer controlled by a SSC-5200 disk station. Dynamic mechanical analysis (DMA) was performed with a heating rate of 10 °C/min at mechanical frequency of 1.00 Hz with a modulation amplitude of 1% length of the sample length using a TA Instruments DMA 2980 dynamic mechanical analyzer. The density of the film was measured using a sink and float method in a mixture of tetrachloromethane and *n*-heptane at 30 °C. Tensile properties in dried air were tested at a strain of 200%/min with a Shimadzu IM-100 autograph, and those in water were tested at a strain of 160%/min with an Iwamoto Tensile Tester to measure tensile strength, elongation, and Young's modulus. The averaged value for 5−10 specimens was employed.

Enzymatic Degradation. The enzyme used in this study is lipase from *Rhizopus delemar* (specific activity of 702 unit/mg from Seikagaku Kogyo Co., Ltd.). The film specimens (20 mm × 20 mm, 80−120 μm thickness) were placed in a vial containing 10 mL of 1/15 mol phosphate buffer solution (pH 5.0) with and without 600 unit/mL of lipase. The vial was incubated at 37 °C for various periods of time. After incubation, the film was washed with water thoroughly and was dried at 40 °C in vacuo to constant weight. The degree of degradation was calculated as the differences between the dry weight after degradation and the initial weight.

Results and Discussion

Degree of Reaction and Structure of Postpolymerized Films. Figure 2a shows FT-IR spectra for GC14 postpolymerized at 0, 1, 2, and 3 h. Broad absorption due to the hydroxyl group in the vicinity of 3500 cm^{-1} decreased with increasing postpolymerization time, while that due to the methylene group at 2960 cm^{-1} was unchanged. Peak separation of these broad spectra is a useful tool to distinguish the peaks for determining the degree of reaction quantitatively. As shown in Figure 2b, FT-IR spectra between 2250 and 4000 cm^{-1} were separated into six Gaussian peaks which were assigned to be due to the stretching vibration of the hydroxyl group at 3450 and 3300 cm^{-1}, the OH stretching vibration in the dimer of carboxylic acid at 3100 and 2580 cm^{-1}, the C−H stretching vibration of the methylene group at 2960 cm^{-1}, and that of the >CH− group at 2854 cm^{-1}. Peaks around 2357 cm^{-1} are absorption due to carbon dioxide.

The possibility of ring opening of lactone was investigated using an infrared absorption due to a carbonyl stretching vibration. Gluconolactone and a mixture of gluconolactone and citric acid have a sharp absorption peak due to the carbonyl group of lactone at 1733 cm^{-1}. The polymerized sample, as shown in Figure 2c, has a strong absorption peak due to the carbonyl group around 1750 cm^{-1}. This absorption peak is the superimposed one due to the carbonyl stretching vibration of lactone at 1733 cm^{-1} and to that of the linear ester linkage at 1788 cm^{-1}. The absorption intensity at 1733 cm^{-1}, due to the carbonyl group of lactone, was not changed upon progress of reaction, but that at 1788 cm^{-1} was increased with progress of reaction and leveled out. These changes of infrared absorption suggest that the ring-opening possibility is very low for the present systems. Therefore, polymerization preferentially occurs through the esterification reaction between the hydroxyl group of G or C and the carboxylic acid of C.

Because the postpolymerization proceeds through the reactions between the hydroxyl group of G or C and the carboxyl acid group of C, the change of absorbance ratio between $^-$OH at 3450 cm^{-1} and >CH_2 at 2960 cm^{-1}, A_{OH}/A_{CH_2}, is a measure of the degree of the reaction. Absorbance due to the hydroxyl group at 3450 cm^{-1}, A_{OH}, was determined by the summation of absorbance of separated peaks at 3450 and 3300 cm^{-1}. Absorbance due to the methylene group, A_{CH_2}, was determined by that of the separated peak at 2960 cm^{-1}. To obtain the quantitative [OH]/[CH_2] ratio in films, the calibration curve between A_{OH}/A_{CH_2} made by the known diols and alcohols was used.[20]

The following equation is defined:

$$\frac{[OH]}{[CH_2]} = \frac{a - y}{b} \tag{1}$$

Here, a is the total number of hydroxyl groups in the monomeric unit at the unreacted initial stage, b is the number of methylene groups in the monomeric unit, and y is the number of reacted hydroxyl groups in the

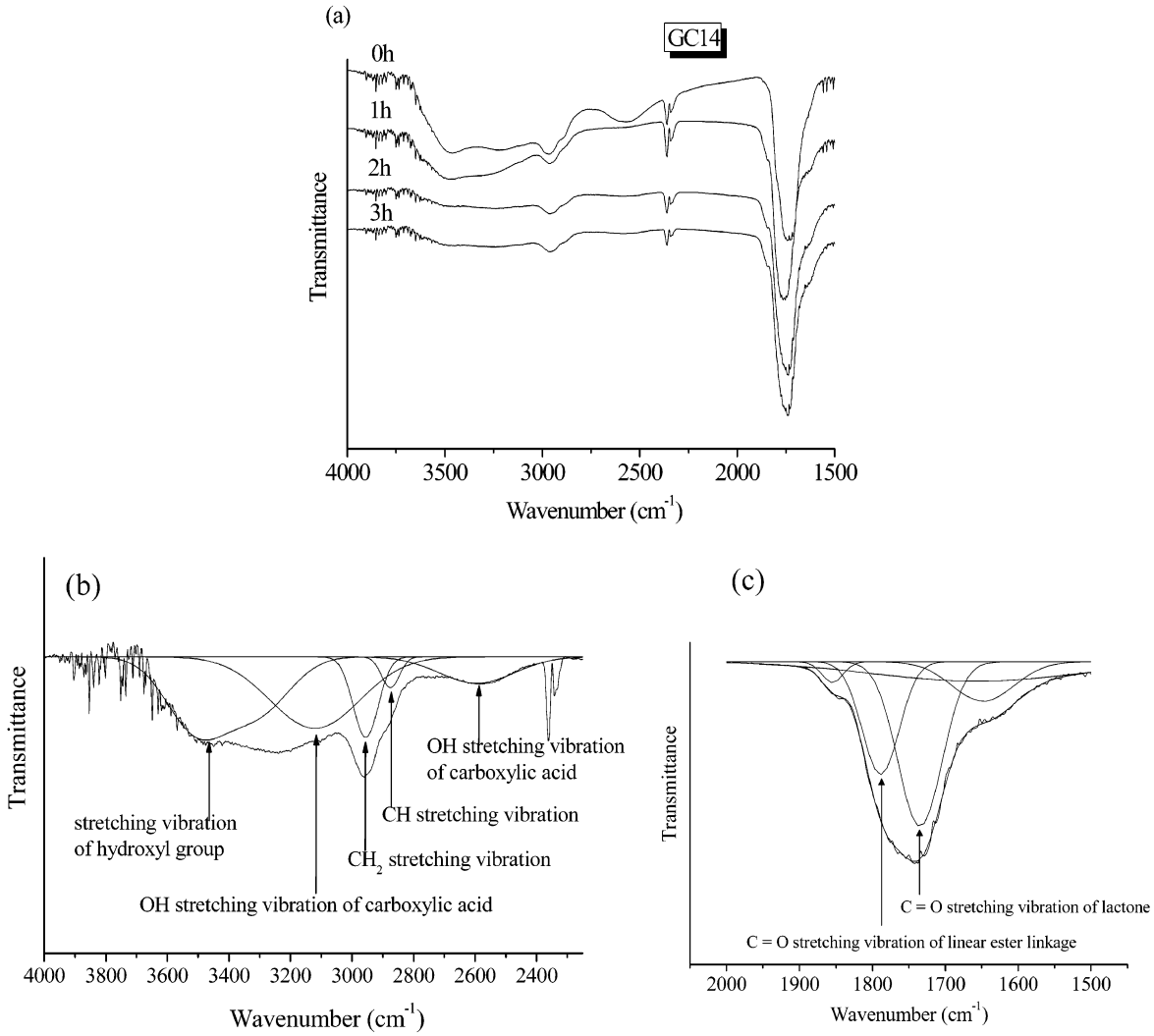

Figure 2. (a) Infrared spectra for GC14 postpolymerized at 180 °C for various periods of time. (b) Peak separation of infrared spectra using the Gaussian peak in the range of 2400−4000 cm^{-1}. (c) Peak separation of infrared spectra using the Gaussian peak in the range of 1500−2000 cm^{-1}.

Table 1. Values of a, b, D_{OH}, D_{OH}', M_C', M_C, ρ, V_f, and Water Absorption for All Polymers

	GC14	GC13	GC12	GC11	GC21	GC31	GC41
a	8	7	6	5	7	7	7
b	9	7	5	3	3.5	3.5	3.5
D_{OH} (%)	66.3	66.8	63.8	52	39.8	37.8	34.7
D_{OH}' (%)	62.5	57	50	40	28.6	28.6	28.6
M_c'	2560	1360	750	660	490		
M_c	9900	8800	6300	6500	4100		
ρ (g/cm^3)	1.342	1.350	1.364	1.367	1.382	1.379	1.380
V_f (cm^3/mol)	0.167	0.160	0.148	0.139	0.123	0.125	0.124
water absorption (%)	20.6	17.8	20.3	18.4	19.8	19.0	22.9

monomeric unit. The degree of reacted hydroxyl group (D_{OH}) is calculated as

$$D_{OH} = \frac{y}{a} \times 100 \qquad (2)$$

In Table 1, a and b values are summarized for all polymers. For GC14, GC13, GC12, and GC11, stoichiometric values of a and b are listed. In the case of GC21, GC31, and GC41, however, $a = 7$ and $b = 3.5$, which are deviated from the stoichiometric values, are listed. The reason is as follows. Figure 3 shows the relation between $[CH_2]/[CH]$ in feed and the absorbance ratio of

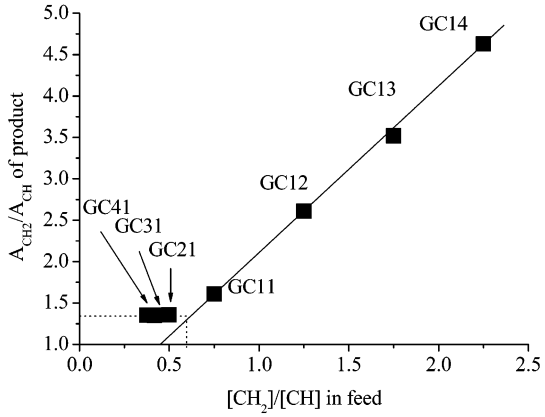

Figure 3. Plots of the absorbance ratio A_{CH_2}/A_{CH} versus $[CH_2]/[CH]$.

A_{CH_2}/A_{CH} measured in the product. Theoretically, the relation should be linear. Indeed, the linear relationship was obtained for GC14, GC13, GC12, and GC11. However, the plots of $[CH_2]/[CH]$ versus A_{CH_2}/A_{CH} deviate from the linear relationship, and the absorbance ratios of A_{CH_2}/A_{CH} measured for GC21, GC31, and GC41 are almost constant. In the case of G rich in feed such as GC21, GC31, and GC41, extra G was unreacted and

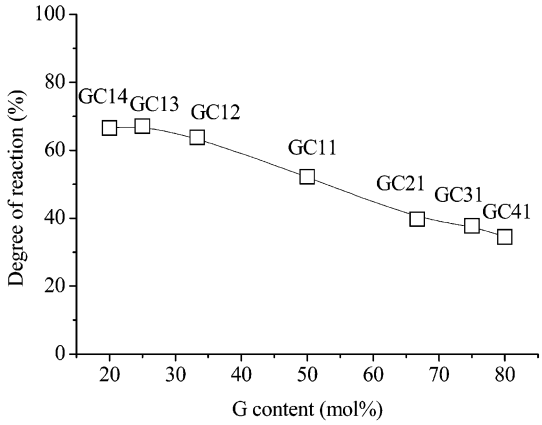

Figure 4. Dependence of the degree of reaction on the G content in the polymer.

might come out from the sample films when they were immersed in hydrochloric solution to dissolve an aluminum substrate. Therefore, an extrapolation value on a linear plot, $[CH_2]/[CH] = 0.58/1$ in feed, was adopted for GC21, GC31, and GC41, from which $a = 7$ and $b = 3.5$ were determined.

The postpolymerization time was determined by the time when the absorption ratio of A_{OH}/A_{CH_2} becomes constant. In the case of complete progress of reaction, GC12 has the stoichiometric molar ratio of G to C in feed to form a complete network. For GC14 and GC13, an extra four and two carboxylic acid groups exist in the monomeric unit, respectively. On the other hand, for GC11, an extra two hydroxyl groups exist in the monomeric unit. In Figure 1b, an example of the network structure of GC11 for complete progress of reaction is illustrated. For GC21, GC31, and GC41, an extra unreacted gluconolactone moiety exists. The degree of reacted hydroxyl group is plotted as a function of G content in Figure 4. In Table 1, the degree of reacted hydroxyl group, D_{OH}, is listed with the degree of reaction, D_{OH}', at which the linear polymers are formed. The degree of reaction at which the linear polymers are formed, D_{OH}', is calculated as follows. Linear GC14 polymer $-(C-G-C-C-C)_n-$ is formed, when five hydroxyl groups in the GC14 monomeric unit are reacted. Next, $D_{OH}' = 5/8 \times 100 = 62.5\%$ is determined. When D_{OH} is larger than D_{OH}', a three-dimensional network is formed. Indeed, it is shown that the relation of $D_{OH} > D_{OH}'$ is satisfied and thus network structures are formed for all postpolymerized polymers. From the values of D_{OH}, D_{OH}', and the molecular weight of each monomeric unit, the average molecular weight between cross-linked sites, the network point (M_c'), was evaluated and listed in Table 1. For example, GC14 polymer has a $-(C-G-C-C-C)-$ monomeric unit, and it's D_{OH} of 66.3% gives the cross-linked (network) site every three monomeric units from which average molecular weight is determined. It is clearly shown that C-rich polymers have a larger network.

Enzymatic Degradability of Postpolymerized Films. Net mass loss due to enzymatic degradation is plotted as a function of incubation time for all polymers in Figure 5. Net mass loss increases with increasing incubation time for GC14, GC13, GC12, and GC11. The dependence of mass loss on G content in feed is shown in Figure 6. GC14 with longer C chains has the largest mass loss. An increase of G content in polymers leads to the decrease of mass loss. Mass loss is plotted against

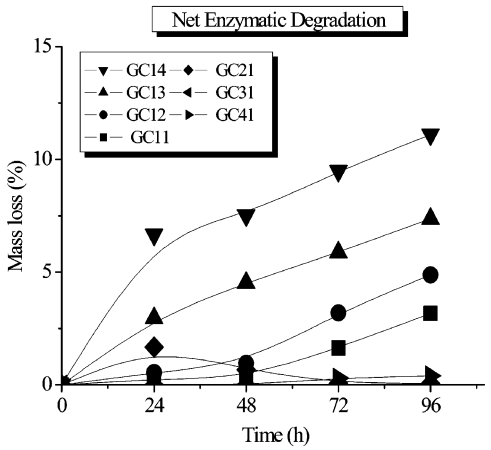

Figure 5. Dependence of net mass loss on the incubation time.

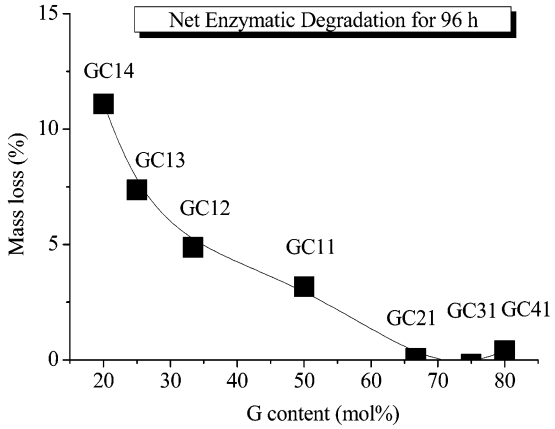

Figure 6. Dependence net mass loss on the G content in the polymer.

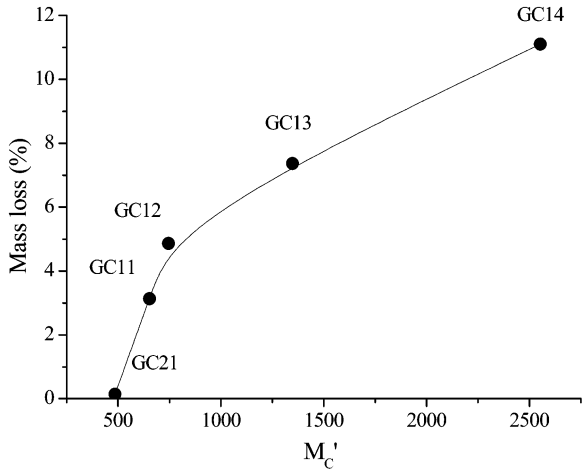

Figure 7. Replots of net mass loss against average molecular weight between cross-linked sites.

the average molecular weight between cross-linked sites M_c' in Figure 7. It is clearly shown that longer M_c' gives larger mass loss due to more favorable enzymatic degradation. An appropriate size of network could accelerate the activation of lipase enzymes. This is consistent with our previous results.[7,8,9,12] Water absorption for each polymer is listed in Table 1. Each polymer has an average water absorption of 20 wt %. These results implied that two or four water molecules had adsorbed to the hydrophilic hydroxyl group with hydrogen bonding.

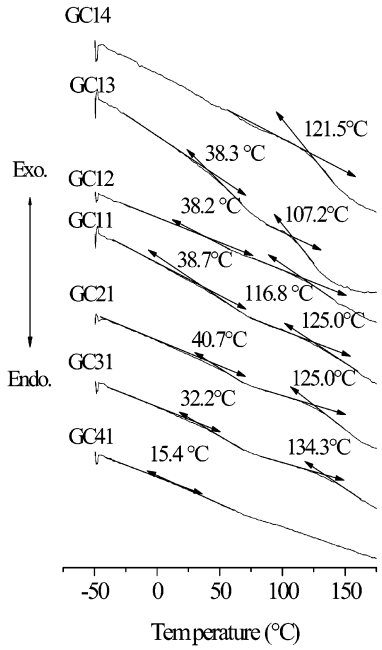

Figure 8. Reversible DSC thermograms of polymers.

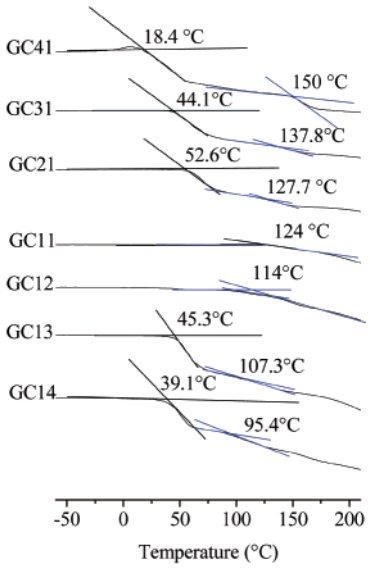

Figure 9. TMA curves of polymers.

Thermal, Mechanical, and Physicochemical Properties of Postpolymerized Films. Broad endothermic peaks appeared on the DSC curves for all polymers. These broad thermograms were separated into reversible and nonreversible mode curves using a modulation technique. Figure 8 shows the DSC thermograms in reversible mode. The resultant reversible thermograms gave two endothermic transitions in the vicinity of 20−40 °C and 105−135 °C for all polymers. Thermomechanical analysis (TMA) also gave the two penetration temperatures as shown in Figure 9, and the higher penetration temperature corresponds to the higher transition temperature measured in modulated DSC. These transitions are ascribed to the transition temperatures due to the relaxation of restricted motion in molecules pinned by the cross-linked sites (amorphous α relaxation). Large penetration occurs at lower temperature in the TMA curve that corresponds to the lower transition temperature in DSC thermograms. The

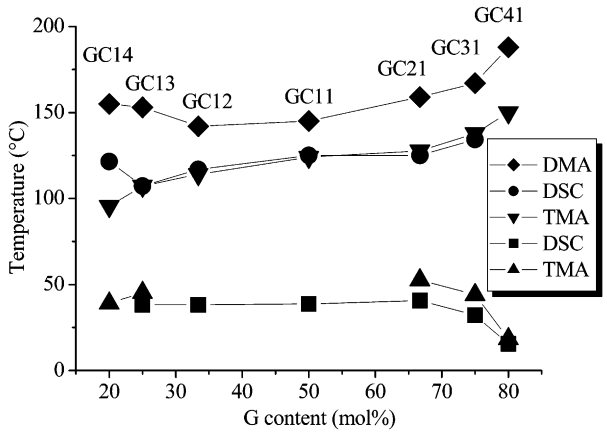

Figure 10. Plots of transition temperatures measured by DMA, DSC, and TMA as a function of G content.

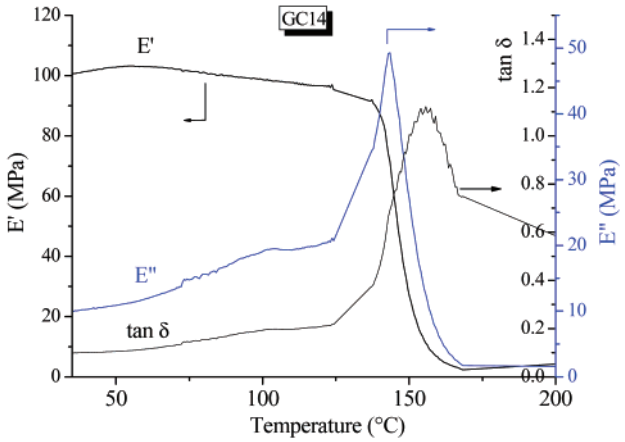

Figure 11. Temperature dependence of storage, loss modulus, and tangent delta.

transitions that appeared at lower temperatures are attributed to the transitions due to the segmental molecular motion of ester linkage (glass transition temperature). These transition temperatures measured by modulated DSC and TMA are plotted as a function of G content in Figure 10. The higher transition temperature due to amorphous α relaxation increases with increasing G content, whereas an almost constant lower transition temperature due to glass transition is measured. The former transition is related to the cross-linked sites, and their increase fashion is consistent with the smaller M_c' value. The latter transition is related to the local segmental motion of the ester linkage, and thus it is almost constant irrespective of the M_c' value.

Figure 11 shows the temperature dependence of the storage modulus as measured by DMA for GC14 film. Dynamic mechanical properties in the rubbery state are sensitive to physical and chemical cross-links. Temperatures at which the maximum tangent delta was measured on DMA were also plotted against G content in Figure 10. The tangent delta peak measured on the DMA curve corresponds to higher transition temperatures on DSC and TMA. The storage modulus becomes flat in a rubbery state as shown in Figure 11. Other films also gave similar behavior. The average molecular weight between cross-linked sites (M_c) is estimated from the equilibrium point in the DMA curve where the

Table 2. Mechanical Properties of All Polymers in Air and in Water at Room Temperature

	GC14	GC13	GC12	GC11	GC21	GC31	GC41
				In Air			
Young's modulus (MPa)	780 ± 50	630 ± 120	970 ± 40	1390 ± 60	1500 ± 330	2140 ± 250	1300 ± 320
tensile strength (MPa)	10 ± 0.5	12.9 ± 0.1	13.5 ± 2.4	15.3 ± 1.8	24.5 ± 1.2	13.2 ± 3.4	14.6 ± 1.4
elongation (%)	2.1 ± 0.1	3.7 ± 1.3	2.4	2.2 ± 0.4	2.5	1.2 ± 0.3	1.5
				In Water			
Young's modulus (MPa)	1.4	1.8	1.0	3.8	5.2	2.1	2.0
tensile strength (MPa)	0.5	0.8	0.8	1.5	2.8	1.5	0.7
elongation (%)	36.7	46.4	78.6	48.1	67.3	80.3	83.4

storage modulus (E_e') becomes flat in a rubbery state, using an equation of

$$E_e' = \frac{3\rho RTe}{M_C}\left(1 - \frac{2M_C}{M}\right) \quad (3)$$

where ρ is the density, R is the gas constant, T_e is the equilibrium temperature, and M is the molecular weight of the polymers. In Table 1, M_c values calculated in the case that infinite network is expanded are listed. As for all polymers, the increase trend of M_c was shown with increasing C content in the network polymer, which is consistent with that of M_c'. An estimation of larger M_c as compared with M_c' may relate to the evaluation of lower E_e' due to the nonuniformity of network formation.

Density increases with increasing G content in the polymeric unit as listed in Table 1. The free volume of the network (V_f) was estimated from the experimentally obtained specific volume V_t (the reciprocal value of measured density (ρ)) and the zero point molar ratio V_0,

$$V_f = V_t - V_0 \quad (4)$$

where V_0 can be calculated from the van der Waals volume V_w of the polymer, $V_0 = 1.3V_w$.[21] V_w is the summation of the group contribution of van der Waals molar volume[22] (cm^3/mol), and M_m is the molecular weight of the repeating monomeric unit. V_f values are also listed in Table 1. Reasonable results are obtained in which the shorter average molecular weight between cross-linked sites M_c' leads to the smaller V_f value.

Mechanical properties in the dried state and in water for all polymers are summarized in Table 2. It is shown that large Young's modulus and tensile strength in the dried state were obtained for GC31 and GC21, respectively. Better mechanical properties, larger Young's modulus and tensile strength, are also significantly related to the smaller average molecular weight between cross-linked sites, M_c'. A large depression of Young's modulus and tensile strength was obtained in water because of plasticization due to absorbed water.

Conclusions

A new type of biodegradable network polyester with considerable enzymatic degradability was prepared from gluconolactone and citric acid with various molar ratios of G and C. Polyesters had considerable water absorbing properties. Enzymatic degradability was determined on the basis of mass loss in a buffer solution with *Rhizopus delemar* lipase. Enzymatic degradability was depressed with a decrease in the content of citric acid in the polymer, which straightly related to the decrease of average molecular weight between cross-linked sites. Two transition temperatures were measured on thermograms in the DSC and TMA curve. Higher transition temperatures were ascribed to the release of restricted motion in molecules pinned by the cross-linked sites. Lower transition temperatures were attributed to the transitions due to the segmental molecular motion of ester linkage. Large Young's modulus and tensile strength in the dried state were obtained for GC31 and GC21, respectively. Absorbed water, which worked as a plasticizer, largely depressed Young's modulus and tensile strength.

References and Notes

(1) Fisher, J. P.; Timmer, M. D.; Holland, T. A.; Dean, D.; Engel, P. S.; Mikos, A. G. *Biomacromolecules* **2003**, *4*, 1327−1334.
(2) Fisher, J. P.; Holland, T. A.; Dean, D.; Mikos, A. G. *Biomacromolecules* **2003**, *4*, 1335−1342.
(3) Behravesh, E.; Jo, S.; Zygourakis, K.; Mikos, A. G. *Biomacromolecules* **2002**, *3*, 374−381.
(4) Timmer, M. D.; Shin, H.; Horch, R. A.; Ambrose, C. G.; Mikos, A. G. *Biomacromolecules* **2003**, *4*, 1026−1033.
(5) Lu, S.; Anseth, K. S. *Macromolecules* **2000**, *33*, 2509−2515.
(6) West, J. L.; Hubbell, J. A. *Macromolecules* **1999**, *32*, 241.
(7) Nagata, M.; Kiyotsukuri, T.; Ibuki, H.; Tsutsumi, N.; Sakai, W. *React. Funct. Polym.* **1996**, *30*, 165−171.
(8) Nagata, M.; Ibuki, H.; Sakai, W.; Tsutsumi, N. *Macromolecules* **1997**, *30*, 6525−6530.
(9) Nagata, M.; Machida, T.; Sakai, W.; Tsutsumi, N. *Macromolecules* **1998**, *31*, 6450−6454.
(10) Nagata, M.; Machida, T.; Sakai, W.; Tsutsumi, N. *J. Polym. Sci., Part A: Polym. Chem.* **1999**, *37*, 2005−2011.
(11) Nagata, M.; Kohno, Y.; Sakai, W.; Tsutsumi, N. *Macromolecules* **1999**, *32*, 7762−7767.
(12) Nagata, M.; Morooka, T.; Sakai, W.; Tsutsumi, N. *J. Polym. Sci., Part A: Polym. Chem.* **2001**, *39*, 2896−2903.
(13) Nagata, M.; Kanechika, M.; Sakai, W.; Tsutsumi, N. *J. Polym. Sci., Part A: Polym. Chem.* **2002**, *40*, 4523−4529.
(14) Kim, D. J.; Kim, W. S.; Lee, D. H.; Min, K. E.; Park, L. S.; Jeon, I. R.; Seo, K. H. *J. Appl. Polym. Sci.* **2001**, *81*, 1115−1124.
(15) Song, C. L.; Yoshii, F.; Kume, T. *J. Macromol. Sci., Pure Appl. Chem.* **2001**, *A38*, 961−971.
(16) Helminen, A.; Korhonen, H.; Seppala, J. V. *Polymer* **2001**, *42*, 3345−3353.
(17) Chung, I.; Xie, D.; Puckett, A. D.; Mays, J. W. *Eur. Polym. J.* **2003**, *39*, 1817−1822.
(18) Schramm, C.; Rinderer, B. *Coloration Technol.* **1999**, *115*, 306−311.
(19) Karadag, E.; Saraydin, D.; Sahiner, N.; Güven, O. *J. Macromol. Sci., Pure Appl. Chem.* **2001**, *38*, 1105−1121.
(20) Tsutsumi, N.; Kiyotsukuri, T.; Chen, Y. *J. Polym. Sci., Part A: Polym. Chem.* **1991**, *29*, 1963−1970.
(21) Bondi, A. *Physical Properties of Molecular Crystals, Liquids and Glasses*; John Wiley & Sons: New York, 1968; Chapters 3 and 4.
(22) Van Krevelen, D. W. *Properties of Polymers*; Elsevier: Amsterdam, 1990; Chapter 4, pp 71−88. The values of group increments of van der Waals volume for V_w estimation are as follows: −COO− 15.2, −OH 8.44, −COOH 18.64, >C< 3.3, >CH− 6.8, −O− 5.0, >C═O 11.7, $-CH_2-$ 10.23 cm^3/mol, respectively.

MA049607G